RSC Advances

ROYAL SOCIETY OF CHEMISTRY

www.rsc.org/advances

RCS Advances

ARTICLE

Non-competitive Inhibitor of Nucleoside Hydrolase from *Leishmania donovani* Identified by Fragment-based Drug Discovery

Received 00th January 20xx,
Accepted 00th January 20xx

DOI: 10.1039/x0xx00000x

www.rsc.org/

M. A. Alves[a,b,c], C. Nirma[a], M. M. Moreira[a], R. O. Soares[d,e], P. G. Pascutti[d,e], F. Noël[b,f], P. R. R. Costa[g], C. M. R. de Sant`Anna[b,h], E. J. Barreiro[b,c], L. M. Lima[b,c], L. W. Tinoco[a*]

Nucleoside hydrolase is an important target for the development of new leishmanicidal agents due its role for parasite proliferation. Using the principles of the fragment-based drug discovery, a library of 111 fragments was assembled for performing a screening by nuclear magnetic resonance using saturation transfer difference. Five fragments were selected as ligands of *Leishmania donovani* nucleoside hydrolase (NH*Ld*) and kinetics studies revealed that fragment **3** acts as a new non-competitive inhibitor. Its binding mode was proposed by molecular docking, using a structural model of NH*Ld* constructed by homology. Intermolecular interaction between fragments **3** and **5** was showed by NOESY and docking studies. These data could be used to design more potent NH*Ld* inhibitors and aid to develop leishmanicidal drugs.

Keywords: Leishmania, nucleoside hydrolase, non-competitive inhibitor, FBDD, STD NMR, molecular docking

1. Introduction

Trypanosomatids represent a family of protozoa that are not able to make the purine synthesis, as other species of microorganisms. The uptake of this auxotrophic nutrient is essential for parasite DNA and RNA biosynthesis and proliferation. This dependence opened an avenue for the development of new antitrypanosomatid agents[1-3].

[a] *Laboratório de Análise e Desenvolvimento de Inibidores Enzimáticos (LADIE), Instituto de Pesquisa em Produtos Naturais (IPPN), Universidade Federal do Rio de Janeiro, 21941-902, Rio de Janeiro, RJ, Brasil.*
[b] *Instituto Nacional de Ciência e Tecnologia de Fármacos e Medicamentos (INCT-INOFAR; http://www.inct-inofar.ccs.ufrj.br/), Laboratório de Avaliação e Síntese de Substâncias Bioativas (LASSBio®), http://www.farmacia.ufrj.br/lassbio/), CCS, Universidade Federal do Rio de Janeiro, Cidade Universitária, P.O. Box 68024, 21941-971, Rio de Janeiro-RJ, Brasil.*
[c] *Programa de Pós-Graduação em Química, Instituto de Química, Universidade Federal do Rio de Janeiro, 21941-902, Rio de Janeiro, RJ, Brasil.*
[d] *Laboratório de Modelagem e Dinâmica Molecular, Instituto de Biofísica Carlos Chagas Filho (IBCCF), Universidade Federal do Rio de Janeiro (UFRJ), Rio de Janeiro, Brasil.*
[e] *Diretoria de Metrologia Aplicada às Ciências da Vida (DIMAV), Instituto Nacional de Metrologia Qualidade e Tecnologia (INMETRO), Xerém, Brasil.*
[f] *Laboratório de Farmacologia Bioquímica e Molecular, Instituto de Ciências Biomédicas-ICB, Universidade Federal do Rio de Janeiro (UFRJ), Rio de Janeiro, Brasil.*
[g] *Laboratório de Química Bioorganica (LQB), Instituto de Pesquisas de Produtos Naturais (IPPN), Universidade Federal do Rio de Janeiro, 21941-902, Rio de Janeiro, RJ, Brasil.*
[h] *Departamento de Química, Instituto de Ciências Exatas, Universidade Federal Rural do Rio de Janeiro (UFRRJ), Seropédica, Brasil.*

**Corresponding author: Prof. Luzineide W. Tinoco, Universidade Federal do Rio de Janeiro, Centro de Ciências da Saúde, Instituto de Pesquisas de Produtos Naturais, Av. Carlos Chagas Filho, 373, Bloco H, LAMAR, Rio de Janeiro, RJ, Brazil, ZIP Code: 21941-902. Phone: +55-21-39386791. Email: lwtinoco@nppn.ufrj.br*

Enzymes involved in the uptake of purines in parasites include purine nucleoside kinases (HGPRTs) and purine ribohydrolases (*i.e.* nucleoside hydrolases, NHs). Among these enzymes, NHs are the most abundant ones. They have been identified and characterized in several microorganisms like *Trypanosoma brucei*, *T. cruzi, T. gondii*, *Leishmania donovani*, *L. mexicana*, *Entamoeba histolytica*, *Escherichia coli*. In these organisms, NHs are glycosidases which act by hydrolyzing *N*-glycosidic bonds of β-ribonucleosides forming nucleic ribose and free bases to be used in purines synthesis[4-6]. Since they are not found in mammals, NHs are considered important targets for the design of selective antiparasitic agents[4, 7-9].

NH of *L. donovani* (NH*Ld*) is a protein with 314 amino acids that shows 96.2% similarity with NH of *L. major*[5]. Different ribohydrolase subtypes are found in trypanosomatids and they differ in their preference or specificity for inosine/uridine substrate. The NH subtypes are highly homologous in their catalytic site, and share similar mechanisms of catalysis.

The early stages of a drug discovery program generally focuses on the identification and optimization of new ligands or leads that can promote inhibition or activation of a protein or pathway, essential for the treatment or cure of a target disease[10,11]. Among the strategies to identify new ligands, the fragment-based drug discovery (FBDD) has been spotlighted in recent years[12]. FBDD is based on the evaluation of the interaction of small molecules (e.g. molecular fragments) with macromolecules (enzymes or receptors), aiming to identify low and medium affinity ligands.

The application of FBDD strategy is supported by the use of methodologies such as Surface Plasmon Resonance[13], Thermophoresis[14], Mass Spectrometry[15] and Nuclear Magnetic Resonance[16], which permit a rapid screening of thousands of

compounds (*i.e* fragments), and allow the measurement of their interaction with target proteins[17-19].

This paper describes the identification of a new non-competitive inhibitor of *L. donovani* nucleoside hydrolase, identified by FBDD strategy, and reports its binding mode proposed by docking studies.

2. Results and discussion

Construction of the fragments library

The molecular fragments were selected according to the Rule of Three[20-22], and based on the structure of inosine, the natural substrate of the enzyme. Accordingly, the selected library was constituted by fragments able to mimic the interactions performed by nitrogenous base or ribose subunits, present in the inosine structure. As exemplified in Figure 1, most chemical fragments selected in this study are in accordance with the rule of three, anticipating a large space for chemical transformation into compounds of greater structural complexity.

All 111 samples of fragments were prepared in DMSO-d_6 (1 mM) and analyzed by ^{1}H NMR. The assignment of all hydrogens was performed for each fragment. Based on ^{1}H NMR chemical shift data one spectra database of all fragments was generated. Fragments were separated by groups containing 3-5 compounds targeting the absence of overlapping signals. The simultaneous STD analysis of groups of fragments in one NMR tube leads to a great economy of time and cost with less consumption of the enzyme.

Ligands selection by STD NMR

For the interaction analyses, groups of fragments (1 mM) were prepared in 20 mM phosphate buffer pH 7.4, 300 mM NaCl, and 10% D_2O. The target protein NH*Ld* was added for a final concentration of 100 µM.

Adapting the basic sequence described by Meyer and Meyer [22] and using the sequence DPFGSE[24] to suppress the water signal, parameters such as pulse power and saturation time were adjusted in the STD control spectra (in the absence of protein) to minimize peaks due to artifacts. Doing so, we ensure that all signals in the STD spectra in the presence of the protein corresponded to the hydrogens in the structure of the ligand involved in the interaction with the protein. These hydrogens have suffered interference of protein magnetization, induced by NMR radio frequency pulse, due to interaction with the macromolecule, a process that allows the characterization of epitopes groups.

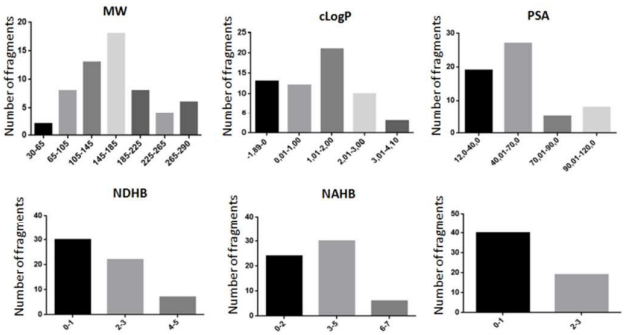

Figure 1. Profile of fragments library. Molecular weight (MW); calculated Partition coefficient (cLog P); Polar surface area (PSA); Number of donor hydrogen bond atoms (NDHB); Number of acceptors hydrogen bond atoms (NAHB); Number of aromatic rings (NAR).

Figure 2 shows an example of the ligand selection process by STD NMR from a mixture of fragments. Based on chemical shifts of the hydrogens of each fragment contained in the mixture, it was possible to identify the ligand fragment in the STD spectra (Figure 2, C), and to determine the epitope groups interacting with the target protein. STD NMR spectra in the absence of protein were used as controls (Figure 2, B), avoiding the selection of false positives due artifacts peaks with the same chemical shift of epitopes groups. Figure 2 illustrates how fragment 1 and fragment 2 were selected as ligands of NH*Ld* and indicates their epitope groups. In order to characterize more precisely signals of the epitope groups, STD spectra were repeated with each active fragment separately, as shown in Figure 3.

Using this methodology, it was possible to identify five fragments that interact with NH*Ld* (Figure 4). Knowing that the shorter is the distance of the connection between ligand and protein, the higher is the signal found in the STD spectrum, the intensity of this signal was normalized, adopting the value of 100% for the strongest signal. This procedure allowed us to map the chemical space of the hydrogens of the ligands participating in the interaction and to classify these epitopes quantitatively, in percentage terms.

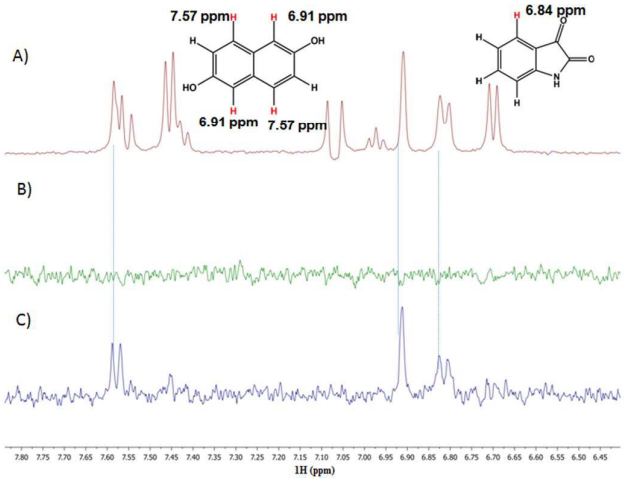

Figure 2. Identification of ligands in a mixture of fragments by STD in phosphate buffer saline pH 7.4 with 10% D_2O. A) ^{1}H NMR

spectrum of the mixture of fragments; B) STD spectrum of fragments mixture without protein (control); C) STD spectrum of the fragments mixture with protein. Epitopes groups are enlightened in red.

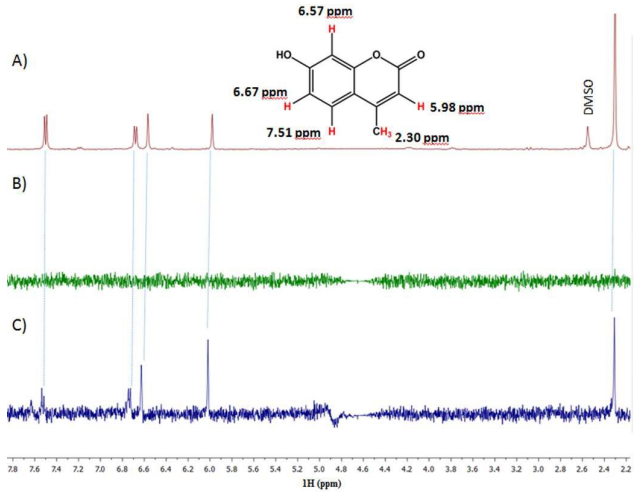

Figure 3. Characterization of epitope groups of Fragment **3** with NH*Ld* protein. A) ^{1}H NMR spectrum in phosphate buffered saline pH 7.4 with 10% D_2O and Fragment **3** (1 mM); B) STD NMR spectrum in phosphate buffered saline pH 7.4 with 10% D_2O and Fragment **3** (1mM) without protein; C) STD NMR spectrum in phosphate buffered saline pH 7.4 with 10% D_2O and Fragment **3** (1mM) in the presence of the protein. The epitopes groups are enlightened in red.

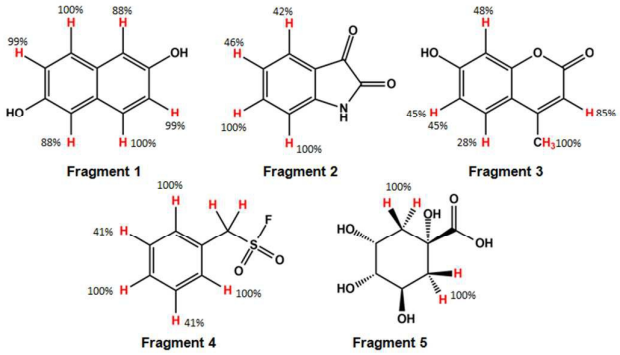

Figure 4. Mapping of epitope groups (in red) of the fragments selected by STD NMR study as ligands of NH*Ld* and STD factor.

NHLd Inhibition assays

Determination of fragments inhibitory activity on NH*Ld*. To identify if fragments selected by STD were able to inhibit NH*Ld* activity, we optimized the enzyme inhibition assay described by Rennó and collaborators[25] and used a fixed concentration of 1 mM fragment and 2 µg/mL NH*Ld*. The uric acid formed by catalysis of the substrate inosine (0.5mM) after conversion of hypoxanthine by the auxiliary enzyme xanthine oxidase was measured. The percentages of inhibition obtained at the screening concentration (1 mM) are showed in Supplementary Information (Table S1) for the five fragments selected by the STD methodology. Compounds that were able to inhibit the NH*Ld* activity by a percentage ≥50% (fragments **1** and **3**) were further analyzed by performing full concentration-effect curves in order to determine the IC_{50} and K_i values. Results indicate that fragments **1** and **3** have significant potencies characterized by IC_{50} values of 525 (K_i= 410) and 294 (K_i=260) µM, respectively. These fragments could be used as starting points for further design of more potent NH*Ld* inhibitors.

Kinetics studies. Drugs or compounds that act as enzyme inhibitors can interact in a reversible or irreversible manner with specific conformational form of the target enzyme[26]. The reversibility of the inhibition produced by the most potent NH*Ld* inhibitor (*i.e.* fragment **3**), was studied for the two possible equilibrium complexes: enzyme-inhibitor complex (EI) and enzyme-substrate-inhibitor (ESI). After an equilibrium period favoring the formation of complex ESI or EI, a jump dilution was performed and the recovery of the enzymatic activity was evaluated for a period of 10 minutes and compared to the control in the absence of the inhibitor during the equilibrium period. The results are depicted in Figure 5. Note that in both cases, the velocity of the enzymatic reaction after dilution of the preformed complex with fragment **3** was similar to the rate of the control reaction, performed in exactly the same conditions but without the inhibitor, indicating a very fast recovery of the enzyme and the reversibility of enzyme inhibition.

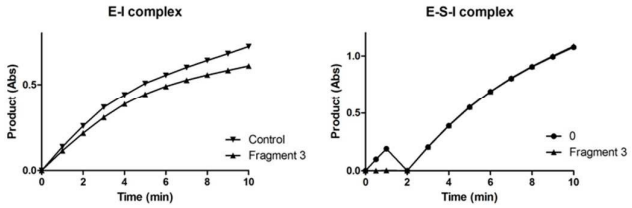

Figure 5. Recovery of NH*Ld* activity after a "jump dilution" of the EI and ESI complex. Fragment **3** (2.9 mM; 10x [IC_{50}]) was present or not (control) during the 20 min pre-incubation period in (20 min for EI complex and 2 min for ESI complex) preceeding the dilution of the inhibitor (see methods for details).). In both cases, time zero indicates the starting time of the enzymatic reaction. For study of the E-I complex, the reaction was started by addition of the substrate 20 min after pre-incubation of fragment 3 with the enzyme. For study of the E-I complex, the reaction was started by addition of the substrate to the medium containing fragment 3 and

the enzyme. After 1 min (peak of absorbance in the control), the mixture was diluted with the same medium but without fragment 3, in order to promote a 10 times dilution of the inhibitor. Note that the product of the reaction was also diluted explaining the decrease in absorbance measured at 2 min (control: first lecture after the dilution).

In order to further characterize the mechanism of inhibition of the NH*Ld* by fragment **3**, we determined which of the four classical models of inhibition better describes the data, obtained using six different concentrations of the substrate inosine, in the absence or in the presence of three different concentrations of fragment **3**[27]. Visual analysis of the data exhibited in Figure 6 shows a decrease of V_{max} in the presence of high concentrations of the inhibitor, so that a competitive mechanism of inhibition was discarded. We used a non-linear regression method considering all the data simultaneously in order to discriminate between the possible mechanisms and to allow a quantitative analysis of the different parameters. The model of non-competitive inhibition was better than the models of uncompetitive and mixed inhibition, as statistically determined by the Aikake criteria. The global fitting of the data using the model of non-competitive inhibition (Figure 6) lead to the determination of the following parameters: V_{max} (mM/min): 234 ± 0.5; K_m (mM): 0.166± 0.002 and K_i: 251± 1 µM. Note also that such methodology is free of the statistical bias inherent in linear transformations of the Michaelis-Menten equation such as in the Lineweaver-Burk plot [27, 28]. Based on these results fragment **3** was identified as a new non-competitive inhibitor of NH*Ld.*

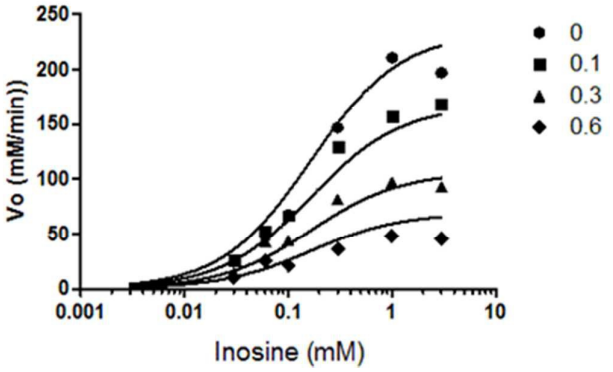

Figure 6. Concentration-effect curves for the activation of NH*Ld* by inosine in the presence of fragment **3**. The experiment was performed in the absence (control, •) or presence of increasing concentrations of fragment **3** (■, 0.1 mM; ▲, 0.3 mM; ♦, 0.6 mM).

NOESY and molecular docking studies

To obtain evidences that can further help in the design of compounds with greater structural complexity and better affinity for NH*Ld,* we consider the possibility of combining the fragment **3**, which displayed the best inhibitory activity (higher potency), with the fragment **5**, a polihydroxyl ligand able to mimic ribose subunit presented in the inosine structure. Therefore, NOESY experiments were conducted to evaluate the spatial proximity between the selected fragments in the presence of NH*Ld*.

In addition to the correlations for the intramolecular spatial of interactions, two regions of spatial intermolecular interactions were also identified and are represented in Supplementary Information (Figure S1-S3). These results indicate that fragments **3** and **5** could interact in regions in close proximity, usually less than 5Å, in the NH*Ld* protein.

Following, a molecular docking study was performed, aiming to establish the binding mode of these fragments with the NH*Ld*. A structural model of NH*Ld* was constructed by homology using the SWISS-MODEL program[29]. Among the templates of nucleoside hydrolases (NH) suggested by the server containing inosine as substrate, the crystal structure of NH *Escherichia coli* (NH*Ec*) was selected, due its higher confidence range (0.97 between changes 1 – 0.09), and its high sequence similarity with the NH*Ld* (i.e. 89%).

The shape complementarity of the experimental structure and the NH*Ld* model was verified through their superimposition in Pymol 1.5.0.5 and obtainment of a RMS value of 0.143. The Ramachandran[30] plot of the best model showed that 93.5% of the residues were in the most favored region, 2.6% were in additional allowed regions, 3.9% were in generously allowed regions and no residues were in disallowed regions (data not shown).

Based upon NMR results, we used a model of the monomeric structure of NH*Ld* to identify the molecular contact surface between NH*Ld* and fragments **3** and **5**. The molecular docking analyses were divided according to the two main purposes. First to determine where fragment **3** interacts with the NH*Ld* monomer, both in inosine-bound and apo form (Figure 7). Second, to evaluate the interactions between the fragment **5** and the fragment**3**-NH*Ld* complex both in inosine-bound and inosine-free forms (Figure 8).

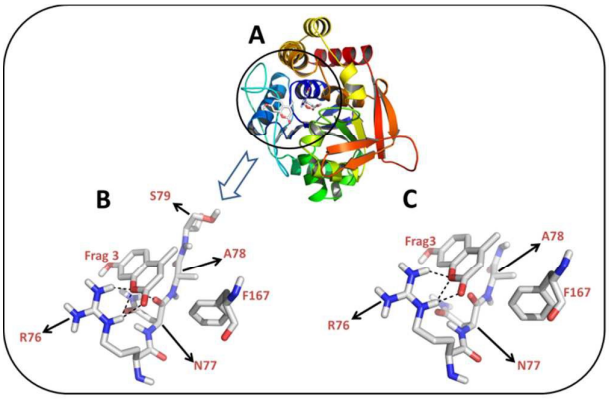

Figure 7. Docking of fragment **3** into NH*Ld* and NH*Ld*-substrate complex. (**A**) Cartoon representation of NH*Ld* containing substrate and fragment **3** (sticks representation). The backbone was colored with rainbow scheme, ranging from blue (N terminal) to red (C terminal). Circle highlights the best binding mode of fragment **3**. (**B**) The best docked conformation of fragment **3** in inosine-bound NH*Ld*. (**C**) The best docked conformation of fragment **3** in NH*Ld* free. Fragment **3** (Frag 3) and residues of the NHLd within 4 Å of the

fragment 3 are indicated by arrow and displayed using stick representation in B and C. Dashed lines represent hydrogen bonds.

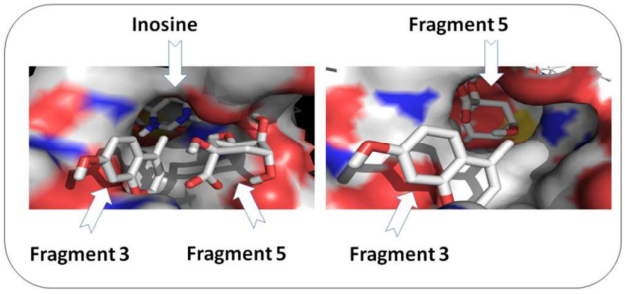

Figure 8. Docking of fragment **5** with NH*Ld*. (**A**) Best pose obtained by docking onto NH*Ld*/inosine/fragment-**3** complex. (**B**) Best pose obtained by docking onto NH*Ld*/fragment-**3** complex. The enzyme in the background is showed as surface map representation. Inosine and fragments **3** and **5** are indicated by arrow and displayed using stick representation. NH*Ld* and fragments were colored by the element (carbon - *gray*, hydrogen - *white*, nitrogen - *blue*, oxygen – *red*, sulfur - *yellow*).

Docking results obtained in the first step indicated that the intermolecular energy (ligand-protein interaction energy based on dispersion repulsion, hydrogen bonding, electrostatics, desolvation, and electrostatics term) for the complex between NH*Ld* and fragment **3** would range between -4.35 and -3.9 kcal/mol, and can be observed in Supplementary Information (Table S2). In about 90% of the poses, there were hydrogen bonds involving the residue Arg76 side chain of NH*Ld*, regardless if the enzyme was complexed or not with the inosine molecule (Figure 7B e 7C). Furthermore, in both complexes, the residues that interact with the fragment 3 are similar (Arg76, Arg77, Ala78, Phe167), the only exception was Ser79 that made contact solely in the presence of inosine (Figure 7B e 7C). Since there is at least partial occupancy by fragment 3 in the active site gate (Figure 8A and 8B), the pocket opening volume for both apo NH*Ld* and fragmente3-bound form were calculated using MOLE 2.0 server[31]. The volume of the cavity for apo form was 4003 Å3 and for fragmente3-bound form was 3955 Å3. The decrease in the volume suggests that fragment 3 blocks the pocket opening, preventing the substrate entry.

Our NMR results indicate that fragments **3** and **5** could bind into NH*Ld* close to each other in the active site. Furthermore, the docking studies suggest that whereas fragment **3** binds in the gate region, fragment **5** is able to establish interactions inside the active site. Based on these results, our research group is now working on the design of different connectors to link fragments **3** and **5**, aiming the discovery of new potent inhibitors of NH*Ld*.

3.Experimental session

Materials

Reagents used in this work, such as inosine and purified xanthine oxidase (XO), were commercially obtained from Sigma-Aldrich®, and have high purity. Fragments included in the library used here were selected from our laboratory or provided by our collaborators. GenScript® synthesized the plasmid used for NH*Ld* expression.

Methods

Fragments library. According to the Rule of Three[20], fragments should be structurally simple molecules, with few functional groups, must have a molecular weight less than 300, a number of donors and hydrogen bond acceptors not higher than three, and a cLogP minor or equal to three.

In addition to these criteria, fragments with some structural similarity with the enzyme substrate inosine were preferentially selected. Fragments were selected for having functional groups that mimic donor and acceptor groups of hydrogen bond, aromatic subunit and for being polyhydroxylated, mimicking nitrogenous base and riboside present in the enzyme substrate.

Expression and purification of *L. donovani* nucleoside hydrolase (NH*Ld*). *L. donovani* nucleoside hydrolase gene (GenBank: AY007193.1) was cloned in pET-28b(+) by NcoI and XhoI to express the recombinant enzyme nucleoside hydrolase *L. donovani* (NH*Ld*) containing a tail of six histidine residues at the C-terminus. The recombinant protein was expressed in *E coli* BL21(DE3) cells and purified by chromatography using nickel affinity column (Ni Sepharose 6 Fast Flow, GE Helthcare®), eluted with 20 mM phosphate buffer pH 7.4, 500 mM NaCl and 300 mM imidazole.

Imidazole was removed (<0.01mM) by washes with 20mM phosphate buffer at pH 7.4 and 300 mM NaCl in Stirred Ultrafiltration Cell System model 8200 Millipore or Amicon® Ultra Centrifugal, with 3.000 MWCO filters. Protein samples were concentrated and quantified by the Lowry method[31], before storage at -80°C.

NMR analysis. All NMR spectra were acquired at 25°C on a 500 VNMRS (Agilent) at 499.78 MHz for ^{1}H and processed with the MestReNova 9.0.1 program. STD spectra were acquired using the basic pulse sequence described by Mayer and Meyer [23], with the inclusion of the Double Pulsed Field Gradient Spin Echo (DPFGSE) [24] for water suppression. Spectra subtraction was performed on alternate scans, producing the difference spectrum. Two seconds were used for saturation transfer with irradiation on-resonance at -2020.5 Hz and off-resonance at 15790.9 Hz and spectra were acquired with 1024 scans. 2D NOESY spectra were acquired with the DPFGSE pulse sequence for water suppression, 1 second mixing time, 64 scans, 1202 points in f2 and 128 in f1.

NMR samples. All 111 molecular fragments at 1mM in DMSO_d_6 were first analyzed by ^{1}H NMR. Mixtures of fragments (3 to 5) were prepared at 1 mM in 20 mM phosphate buffer pH 7.4 containing 300 mM NaCl and 10% D_2O. ^{1}H NMR spectra were acquired for each fragment mixture sample. For STD binding assays, the protein, NH*Ld* (100 µM), was added to the medium for obtaining a molar ratio of 100:1 (fragment:protein).

Analysis of steady-state enzyme inhibition. Kinetics parameters of NH*Ld* were determined adapting the methodology described by Rennó and collaborators[25] to 96 well plates and measuring the

enzyme kinetics using the spectrophotometric system SpectraMax M5 Molecular Devices® Microplate Reader. We used a coupled optical assay with the auxiliary enzyme xanthine oxidase (XO, 93 µg/mL) in 20 mM phosphate buffer pH7.4 containing 300 mM NaCl and 0.5 mM inosine. The reaction was started by addition of 2 µg/mL NH*Ld*. The product (uric acid) formation was monitored at 293 nm in a final volume of 300 µL. All experiments were performed in triplicate at room temperature. The kinetics parameters Michaelis-Menten constant (K_m) and maximum velocity (V_{max}) were evaluated by increasing the concentration of inosine from 0.1 to 1mM, to obtain data above and below the K_m maintaining constant the concentration of NH*Ld* (2 µg/mL). The saturation curve was obtained by plotting the values of initial rate *versus* substrate concentration and analyzed by nonlinear regression (GraphPad Prism 5.0 software) using the Michaelis-Menten equation: $V_0 = V_{max} * [S] / ([S] + K_m)$, where [S] is the substrate concentration, V_{max} is the maximum velocity and K_m is the Michaelis-Menten constant.

Fragments selected by STD were first screened at 1 mM for their inhibition of NH*Ld* activity using the procedure described above with fixed concentrations of inosine (0.5 mM) and enzyme (2 µg/mL). Fragments that inhibited more than 50% of the enzyme activity were selected for IC_{50} determination. IC_{50} were determined using at least 6 concentrations of inhibitor and fixed concentrations of enzyme (2 µg/mL) and inosine (0.5 mM). IC_{50} values were obtained by nonlinear regression analysis (GraphPad Prism 5.0). K_i values were determined using the Cheng-Prussof equation: $Ki = [IC_{50} / (1+ [S] / K_m)]$ [26]. The reversibility of the enzymatic inhibition was analyzed for the complex E-I and E-S-I [26].

The complex E-I was evaluated by pre-incubating the fragments at concentrations 10 times higher than their IC_{50} together with 0.2 mg/mL NH*Ld* (100 times higher than the usual concentration for incubation) in phosphate buffer (20 mM pH 7.4, 300 mM NaCl). After 20 minutes, a "jump dilution" was done and the reaction was started by adding the phosphate buffer containing XO (93 µg/mL) and inosine (0.3mM) in order to promote a 100 times dilution of both fragments and enzyme.

The complex E-S-I was evaluated by adding the usual concentrations of enzyme, inosine, XO, and the fragment (at a concentration equal to its IC_{50}). After the complex E-S-I formation (~1min), the medium was diluted 10 times with the same solution but without the fragment, in order to promote a 10 times dilution of the inhibitor. In both experiments, the reversibility of the inhibition was assessed measuring the recovery of the enzymatic activity in comparison with control samples without inhibitor during the pre-incubation step.

The same experimental conditions were used to determine the type of enzymatic inhibition. In this case, five concentrations of inosine (0.03, 0.1, 0.3, 1, 3 mM) were used in the absence (control) and presence of three fixed concentrations of the inhibitor (100, 300 and 600 µM), selected according to the IC_{50}. The whole data (from the four curves) were simultaneously analyzed by non-linear regression in order to compare different classical models of inhibition and to choose the best one using the Aikake criteria (GarphPad Prism version 5.0).

Molecular modelling. The three-dimensional model of the NH*Ld* was obtained based on the structure of the nucleoside hydrolase of *E. coli* (access code 3B9X, 2.3 Å of resolution, in Protein Data Bank – PDB) [32], which has 89% sequence similarity[33] with the NH*Ld.* This structure was chosen because it was solved with the substrate inosine, different from the model previously described by Tanos and collaborators[34]. We used the T-Coffee server[35] to align the template and the NH*Ld*. Then, the model building was performed submitting the alignment to the SWISSMODEL server [29]. Model validation using Ramachandran plot was performed by the server Rampage [30].

Molecular docking. Fragments were drawn using the PC Spartan´14 package and their binding modes (ligand-target) were investigated by docking methodology implemented in AutoDock4.2[36]. The graphical interface AutoDock Tools was used to prepare and analyze the docking [36]. The enzyme was kept fixed and the docking calculations were performed by using a grid map of 60 x 50 x 60 points centered in the calcium atom, with a grid spacing of 0.375 A. Since ligands are not peptides, the Gasteiger-Marsile charge was assigned[37] and then non-polar hydrogens were merged. Docking runs were performed using the Lamarckian Genetic Algorithm[38] and remaining parameters were set as default values.

Conclusions

We performed a screening analysis of 111 fragments on NH*Ld* using saturation transfer difference (STD) NMR spectroscopy. From this analysis, five fragments were selected as ligands of the target enzyme, and their ability to inhibit enzymatic activity of NH*Ld* was investigated. Fragments **1** and **3** stood out showing IC_{50} values of 525 µM and 294 µM, respectively. The mechanism of inhibition of fragment **3** was determined, revealing the identification of a new non-competitive inhibitor of NH*Ld*. Its binding mode was proposed by molecular docking, using a structural model of NH*Ld* constructed by homology. NOESY and comparative docking studies between fragments **3** and **5** were established and the results will be used in the design of more potent NH*Ld* inhibitors.

Acknowledgments

Authors would like to thank CNPq (BR), CAPES (BR), FAPERJ (BR) and INCT-INOFAR (BR, 573.564/2008-6 and E-26/170.020/2008) for fellowship and financial support.

Author Contributions

Conceived and designed the experiments: MAM, LML, FN EJB, PGP, LWT. Performed the experiments: MAM, CN, MMM, ROS. Analyzed the data: MAM, FN, CMRS, LWT. Contributed reagents/materials/analysis tools: EJB, LML, PGP, PRRC, LWT. Wrote the paper: MAM, ROS, CMRS, FN, LML, LWT.

Disclosure

Authors report no conflicts of interest in this work.

References

1. P. Y. Nicola, S. Carter, A. S. Cassandra, B. M. Jan, U. Buddy, *Drug Targets in Kinetoplastid Parasites*, Springer New York, 2008, 141-154.
2. M. Berg, P. V. D. Veken, A. Goeminne, A. Haemers, K. Augustyns, *Curr. Med. Chem.*, 2010, **17**, 2456-2481.
3. A. K. Datta, R. Datta, B. Sen, *Drug Targets in Kinetoplastid Parasites*, ed. H. K. Majumder, Springer New York, New York, NY, 2008, 116-132.
4. M. Santana, G. P. Borja-Cabrera, E. Paraguai de Souza, N. R. Sturm, C. B. Palatnik de Sousa, D. A. Campbell, *Mol. Biochem. Parasitol.*, 2002, **120**, 315-319.
5. L. Cui, G. R. Rajasekariah, S. K. Martin, *Gene*, 2001, **280**, 153-162.
6. W. Versées and J. Steyaert, *Curr. Opin. Struct. Biol.,* 2003, **13**, 731-738.
7. N. Carter, P. Yates, C. Arendt, J. Boitz and B. Ullman, *Adv. Exp. Med. Biol.*, 2008, **625**, 141-154.
8. D. Nico, D. C. Gomes, I. Palatnik-de-Sousa, A. Morrot, M. Palatnik and C. B. Palatnik-de-Sousa, *Front. Immunol.*, 2014, **5**, 273.
9. W. Barnali, G. Ambarnil, B. Dhananjay, G. Nanda, B. Rahul, *BMC Res. Notes*, 2014, **7**, 802
10. R. V. C. Guido, A. D. Andricopulo and G. Oliva*, Estudos Avançados, 201*0, **24**, 81-98.
11. J. P. Hughes, S. Rees, S. B. Kalindjian and K. L. Philpott, *Br. J. Pharmacol.*, 2011, **162**, 1239-1249.
12. O. Rabal, M. Urbano-Cuadrado and J. Oyarzabal, *Future Med. Chem.*, 2010, **3**, 95-134.
13. S. Perspicace, D. Banner, J. r. Benz, F. Muller, D. Schlatter and W. Huber, *J. of Biomol. Screening*, 2009, **14**, 337-349.
14. S. A. I. Seidel, C. J. Wienken, S. Geissler, M. Jerabek-Willemsen, S. Duhr, A. Reiter, D. Trauner, D. Braun and P. Baaske, *Angew. Chem. Int. Ed.*, 2012, **51**, 10656-10659.
15. V. Vivat Hannah, C. Atmanene, D. Zeyer, A. Van Dorsselaer and S. Sanglier-Cianférani, *Future Med. Chem.*, 2009, **2**, 35-50.
16. M. J. Harner, A. O. Frank and S. W. Fesik, *J. Biomol. NMR*, 2013, **56**, 65-75.
17. G. de Kloe, D. Bailey, R. Leurs and I. de Esch, *Drug Discovery Today*, 2009, **14**, 630-646.
18. P. Hajduk and J. Greer, *Nat. Rev. Drug Discovery*, 2007, **6**, 211-219.
19. S. J. Pfaff, M. S. Chimenti, M. J. S. Kelly and M. R. Arkin, in *Protein-Protein Interactions: Methods and Applications*, eds. L. C. Meyerkord and H. Fu, Springer New York, New York, NY, DOI: 10.1007/978-1-4939-2425-7_39, pp. 587-613.
20. M. Congreve, R. Carr, C. Murray and H. Jhoti, *Drug Discovery Today*, 2003, **8**, 876-877.
21. H. Jhoti, G. Williams, D. C. Rees and C. W. Murray, *Nat. Rev. Drug. Discov.*, 2013, **12**, 644-644.
22. G. M. Keserű, D. A. Erlanson, G. G. Ferenczy, M. M. Hann, C. W. Murray and S. D. Pickett, *J. Med. Chem.*, 2016, DOI: 10.1021/acs.jmedchem.6b00197.
23. M. Mayer, B. Meyer, *J. Am. Chem. Soc.*, 2001, **123**, 6108-6117.
24. C. Dalvit, *J. Biomol. NMR*, 1998, **11**, 437-444.
25. M. N. Rennó, T. C. C. França, D. Nico, C. B. Palatnik-de-Sousa, L. W. Tinoco and J. D. Figueroa-Villar, *Eur. J. Med. Chem.*, 2012, **56**, 301-307.
26. R. A. Copeland, *Evaluation of Enzyme Inhibitors in Drug Discovery: A Guide for Medicinal Chemists and Pharmacologists*, John Wiley & Sons, 2005.
27. C. J. Noel F., *Braz. J. Med. Biol. Res.*, 1989, **22**, 433-445.
28. R. L. A. Motulsky H.J., *FESEB J.*, 1987, **1**, 365-374.
29. M. Biasini, S. Bienert, A. Waterhouse, K. Arnold, G. Studer, T. Schmidt, F. Kiefer, T. G. Cassarino, M. Bertoni, L. Bordoli and T. Schwede, *Nucleic Acids Res.*, 2014, **42**, W252-W258.
30. I. W. D. S. C. Lovell, W. B. Arendall III, P. I. W. de Bakker, J. M. Word, M. G. Prisant, J. S. Richardson and D. C. Richardson, *Proteins: Struct., Funct., Genet.*, 2002, **50**, 437-450.
31. D. Sehnal, R. S. Vareková, K. Berka, L. Pravda, V. Navrátilová, P. Banás, C-M. Ionescu, M. Otyepka, J. Koca, *J. Cheminf.*, 2013, 5: 39-10.
32. O. H. Lowry, N. J. Rosebrough, A. L. Farr and R. J. Randall, *J. Biol. Chem.*, 1951, **193**, 265-275.
33. B. G. E. Lovane, Laura Muzzolini, V. Matafora, A. Fornili, C. Minici, F. Giannese, M.Degano, *Biochemistry*, 2008, **47**, 4418-4426.
34. T.C. C. França, M. R. M. Rocha, B. M. Reboredo, M. N. Rennó, L. W. Tinoco, J. D. Figueroa-Villar, *J. Braz. Chem. Soc.*, 2008, **19**, 64-73.
35. D. G. H. C. Notredame, J. Heringa, *J. Mol. Biol.*, 2000, **302**, 205-217.
36. G. M. Morris, R. Huey, W. Lindstrom, M. F. Sanner, R. K. Belew, D. S. Goodsell and A. J. Olson, *J. Comput. Chem.*, 2009, **30**, 2785-2791.
37. J. Gasteiger, M. Marsili, *Tetrahedron*, 1980, **36**, 3219-3228.
38. G. M. Morris, D. S. Goodsell, R. S. Halliday, R. Huey, W. E. Hart, R. K. Belew, A. J. Olson, *Comput. Chem.,* 1998, **19**, 1639-1662.

New non-competitive inhibitor of nucleoside hidrolase from *L. donovani* identified by fragment-based drug discovery using STD NMR and molecular docking